Asian Journal of Chemistry; Vol. 27, No. 5 (2015), 1621-1625

ASIAN JOURNAL OF CHEMISTRY

http://dx.doi.org/10.14233/ajchem.2015.17395

Surface Initiated ATRP of Acrylic Acid and Acrylamide on Cellulose Acetate Fiber

JIN WANG[1,2], ZHIHUA LIU[1], KUNMIAO WANG[1], PEI HE[1], CHUNBO LIU[1], YONGKUAN CHEN[1,*] and CHUNCHENG LI[2,*]

[1]Yunnan Academy of Tobacco Science, Kunming 650106, Yunnan Province, P.R. China
[2]Beijing National Laboratory for Molecular Sciences, CAS Key Laboratory of Engineering Plastics, Institute of Chemistry, Chinese Academy of Sciences, Beijing 100190, P.R. China

*Corresponding authors: Tel/Fax: +86 871 68319138; E-mail: ykchen@cyats.com, lichch@iccas.ac.cn

Received: 14 February 2014; *Accepted*: 22 April 2014; *Published online*: 20 February 2015; AJC-16855

Using surface initiated atom transfer radical polymerization (ATRP) as grafting method, acrylic acid and acrylamide grafting onto cellulose acetate fiber were successfully carried out. The chemical structures and molecular weights of copolymers were characterized by XPS, ^{1}H NMR and FTIR. The thermal stabilities and topography of copolymers were investigated by TGA and SEM. The kinetics study revealed an approximately linear increase in the graft yield of the poly(acrylic acid) and polyacrylamide with polymerization concentration, indicating that chain growth from the fiber surface was consistent with a controlled process.

Keywords: Cellulose acetate, Atom transfer radical polymerization, Poly(acrylic acid), Polyacrylamide.

INTRODUCTION

Cellulose, being the most abundant natural polymer, is a highly interesting material due to its renewability, biodegradability and attractive mechanical properties[1-5]. However, cellulose is high crystalloid, strong inter- and intra-molecular hydrogen bonding caused by hydrogen bonding networks, these properties make cellulose cannot be processed by the melt processing, which is the most economical and efficient processing method for polymers. The main disadvantage of cellulose is its poor processability, which restricts the application of cellulose in different fields[6-10]. In order to improve the thermal processibility of cellulose, the most common way is chemical modification, of which esterification is the primary way to expand the utilities of cellulose. Cellulose acetate (CA), as one of the commercially important cellulose esters, is widely used in making fibers, films, coating and molded plastics[11-13]. Due to their very narrow thermal processing window between melt and decomposition temperatures, a lot of low-molecular-weight plasticizers are usually required for cellulose acetate melt processing[10]. The main problem of this method is migration of the external plasticizers, which may lead to changes in long-term material performance and potential health risks[14]. Several studies have focused on graft copolymerization, which can introduce a variety of functional groups to alter the chemical and physical properties of cellulose acetate. For example, Nishio and Teramoto[15,16] grafted cellulose acetate with poly(lactic acid) through ROP of L-lactic acid and found that the obtained graft copolymers exhibited thermoplastic behaviour.

To the best of our knowledge, no attention has been paid to the surface initiated atom transfer radical polymerization (ATRP) grafting acrylic acid and acry-lamide onto cellulose acetate fibers. In this work, we report the synthesis of a series of CA-*g*-PAA and CA-*g*-PAM copoly-mers from cellulose acetate fiber directly by surface-initiated ATRP. The chemical structure, thermal stabilities and topography properties of these copolymers were characterized. The kinetics of ATRP polymerization were also evaluated.

EXPERIMENTAL

Cellulose acetate (CA) fiber was obtained from Kunming Cellulose Fiber Co., Ltd. Acrylic acid (AA) and acrylamide (AM) were from Beijing Chemical Reagent Co., Ltd and acrylic acid distilled under reduced pressure. Copper(I) bromide (CuBr, 98 %) was supplied by Aldrich Chemical Co., dissolved in hydrochloric acid, precipitated into a large amount of deionized water, filtered, washed with anhydrous ethanol and finally dried under reduced pressure at room temperature. 2,2-Dipyridyl was also purchased from Beijing Chemical Reagent Co., Ltd. All other solvents obtained from Fisher Scientific Co. and were used as received.

Surface-initiated ATRP on the cellulose acetate fiber: For the reaction of hydroxyl groups on the cellulose acetate fiber with 2-bromoisobutyryl bromide (BIBB), the fiber was

immersed in the anhydrous toluene solution comprising 2-bromoisobutyryl bromide (BIBB, 10 mM) and triethylamine (10 mM) for 2 h. 2-Bromoisobutyryl bromide (BIBB) reacts with the hydroxyl groups of the cellulose acetate fiber to immobilize bromoester initiator groups covalently to the fiber surface. After the reaction, the initiator-functionalized fiber was removed from the reaction mixture and washed thoroughly with toluene and deionized water before being dried under reduced pressure.

Surface-initiated atom transfer radical polymerization (ATRP) of poly(acrylic acid) and polyacrylamide on the CA-Br fiber was accomplished in a magnetically stirred glass tube (50 mL) by immersing the fiber into a reaction mixture.

The acrylic acid reaction solution comprised the monomer, acrylic acid (2.88 g, 1 mol/L); catalyst, CuBr (2.97 mg), 2,2-dipyridyl (4.68 mg); and 40 mL of deionized water as solvent. Acrylic acid was deprotonated by the addition of NaOH to reach a pH end point of 10.2, followed by the addition of NaCl (5.59 g), according to the protocol first proposed by Sankhe *et al.*[17]. The acrylamide reaction solution comprised the monomer, acrylamide (AM, 2.84 g, 1 mol/L); catalyst, CuBr (2.97 mg), 2,2-dipyridyl (4.68 mg); and 40 mL of deionized water as solvent.

The reaction mixture was purged with argon for 2 h in ice water bath to remove the dissolved oxygen. Polymerization was carried out at 50 °C under argon atmosphere for the desired reaction time. At the end of the reaction, the poly(acrylic acid) (PAA) and polyacrylamide (PAM) graft cellulose acetate fiber (CA-*g*-PAA and CA-*g*-PAM) was subjected to exhaustive washing and extraction with water and ethanol and then dried under reduced pressure at room temperature for at least 24 h until a constant weight was obtained.

The surface chemical composition of the pristine and modified cellulose acetate fiber was characterized by X-ray photoelectron spectroscopy (XPS). The XPS measurements were performed on a kratos AXIS Hsi spectrometer using a AlK_α X-ray source (1486.6 eV photons). The X-ray source was run at a reduced power of 150 W (15 kV and 10 mA). The corelevel spectra were obtained at the photoelectron takeoff angle (a, with respect to the sample surface) of 90°. The pressure in the analysis chamber was maintained at 10^{-8} Torr or lower during each measurement. To compensate for surface charging effects, all binding energies (BE's) were referenced to the C 1s hydrocarbon peak at 284.6 eV. In peak synthesis, the line width (full width at half maximum or FWHM) of Gaussian peaks was maintained constant for all components in a particular spectrum. Surface elemental stoichiometries were determined from the peak area ratios, after correction with the elementally determined sensitivity factors and were accurate to within ±5 %.

The chemical structures and compositions of the obtained cellulose acetate fiber were characterized by a Bruker DMX-400 NMR spectrometer at ambient temperature, using DMSO as the corresponding solvent and tetramethylsilane as the internal chemical shift standard. Fourier transform infrared (FTIR) spectrum was collected in the transmission mode with Nicolet 750 under ambient conditions.

The thermal stability of the polymers was characterized using thermogravimetric analysis (TGA) with a Perkin-Elmer Pyris 1 TGA thermogravimetric analyzer. Samples of 2-3 mg were heated from 50 to 700 °C at a rate of 20 °C min^{-1} in nitrogen atmosphere with a gas flow rate of 20 cm^3 min^{-1}.

The surface morphologies of the cellulose acetate fiber were imaged using a JEOL scanning electron microscope (SEM, model 5600LV). The SEM measurements were performed at an accelerating voltage of 20 kV.

RESULTS AND DISCUSSION

The process of surface graft of cellulose acetate fiber *via* controlled radical polymerization is shown in Fig. 1: (i) the hydroxy groups on the cellulose acetate fiber react with BIBB led to the alkyl halide-functionalized CA-Br fiber (hereafter refer to the CA-Br fiber surface) and (iii) consecutive surface-initiated ATRP from the CA-Br fiber (hereafter refer to the CA-*g*-PAA or CA-*g*-PAM surface).

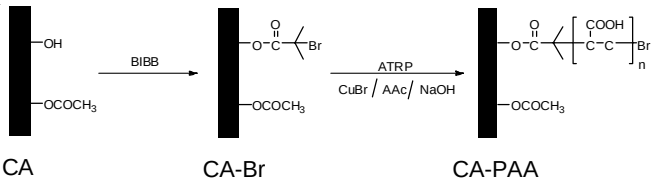

Fig. 1. Schematic diagram illustrating the synthesis routes of CA-Br, CA-*g*-PAA copolymers

Modification and characterization: The physico-chemical properties of the cellulose acetate fiber can be tuned by the grafting of functional polymer. In this work, acrylic acid (AA) was selected as the model monomer for the preparation of functional polymer from the cellulose acetate fiber *via* surface initiated ATRP.

The presence of grafted poly(acrylic acid) on the cellulose acetate fiber surfaces was confirmed by XPS analysis after the surfaces had been subjected to vigorous washing and extraction. Fig. 2 shows the wide scan and C 1s core-level spectra of the cellulose acetate, CA-Br, CA-*g*-PAA (from 3 h of ATRP), respectively.

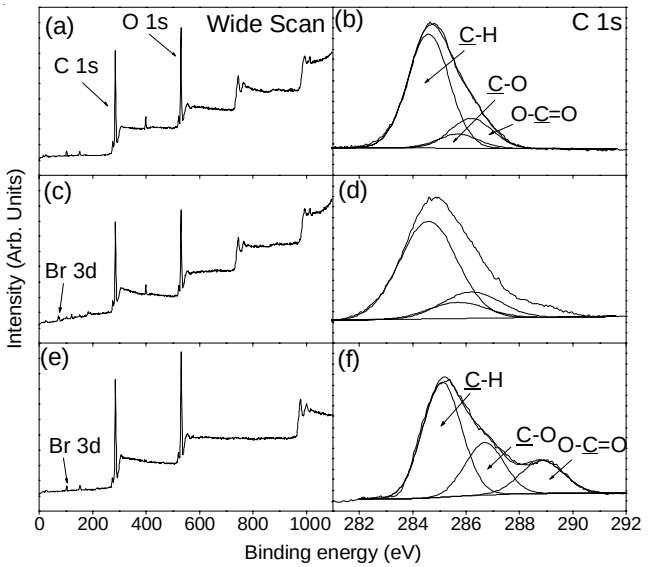

Fig. 2. XPS wide scan and C 1s core level spectra of (a,b) the pristine CA fiber, (c,d) CA-Br, and (c) the CA-*g*-PAA surface

A comparison of the wide-scan spectra of the cellulose acetate [Fig. 2(a)] and CA-Br surfaces [Fig. 2(c)] reveals that the Br 3d (at a BE of about 69 eV), Br 3p (at a BE of about 182 eV) and Br 3s (at a BE of about 256 eV) signals, characteristic of covalently bonded bromine, have appeared on the CA-Br surface. Even after the acrylic acid graft, the Br signals have still appeared on the CA-*g*-PAA surface [Fig. 2(e)]. It indicates that the graft reaction is living polymerization, it retains to initiate monomers grafting.

As shown in Fig. 3(b,d,f), the C 1s core-level spectra of the cellulose acetate, CA-Br, CA-*g*-PAA surfaces can be curve-fitted into three peak components, with BEs at 284.6 for the C-H species, at 286.2 eV for the C-O species and at 288.4 eV for the O-C=O species, respectively. After the acrylic acid graft the area of O-C=O is larger, it because of [C=O]/[C] of acrylic acid is bigger than that of cellulose acetate. It also confirmed that acrylic acid grafted to the surface of cellulose acetate.

The chemical structures were also characterized by ^{1}H NMR. The ^{1}H NMR spectrum of the cellulose acetate, CA-*g*-PAA, CA-*g*-PAM is shown in Fig. 3. The peaks occurring at 1.8-2.2 (δH^a) and 3.5-5.5 (δH^b) ppm are reasonably assigned to different types of methylene protons in the repeating units of cellulose acetate Fig. 3(a). After acrylic acid graft (Fig. 3(b)), the chemical shifts of two kinds of methylene protons of acrylic acid in copolymers molecular chain were observed at 1.7 (δH^1), 2.4 (δH^2) ppm [Fig. 3(b)][18]. And in Fig. 3(c), the acrylamide methylene protons peaks 1.6 (δH^3), 2.1 (δH^4) ppm also appeared in the CA-*g*-PAM[19].

In addition, the chemical structures determined by FTIR were also important to study cellulose acetate, CA-*g*-PAA as well as the CA-*g*-PAM and the results are shown in Fig. 4. In Fig. 4 cellulose acetate's curve, the wide peak around 3500 cm^{-1} assigned to the absorption band of the hydroxyl groups and 1752 cm^{-1} is carbonyl peak of cellulose acetate[10]. After the acrylic acid graft, hydroxyl peaks decreased significantly, indicating that some of the hydroxyl groups were substituted by acetyl groups; And while carbonyl peak of CA-*g*-PAA shifted to 1708 cm^{-1}. After acrylamide grafting, the wide peak around 3400 cm^{-1} become larger, which is N-H stretching vibration peak. At the same time, the 1662 cm^{-1} C=O peak on amide existed. Through the changes of the FTIR spectra, it proved the existence of the graft copolymer.

Therefore, it can be concluded that CA-*g*-PAA, CA-*g*-PAM copolymers were successfully synthesized *via* surface-initiated ATRP on the cellulose acetate fiber on the basis of XPS, NMR and FTIR results.

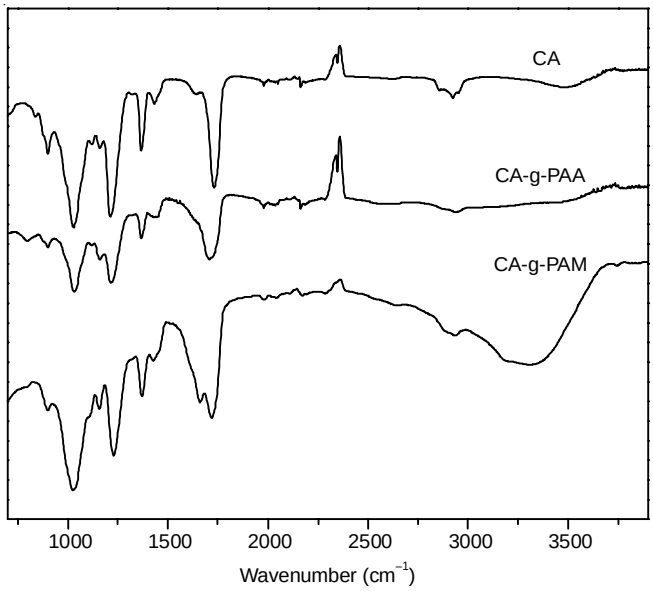

Fig. 4. FTIR spectra of (a) cellulose acetate fiber,(b) the CA-*g*-PAA and (c) CA-*g*-PAM

Surface topography: The surface morphology of the cellulose acetate fiber at various surface modification was studied by SEM. Fig. 5 shows the respective SEM images of the pristine cellulose acetate fiber (Fig. 5(a)), CA-*g*-PAA fiber (Fig. 5(b)) and CA-*g*-PAM fiber (Fig. 5(c)). Obviously, the diameter of the cellulose acetate fiber was about 30 μm and the surface of the fiber is smooth. After acrylic acid and acrylamide graft, there were many particles on the fiber surface, the surface of the fiber became very rough. The SEM images of the fiber also indicated that ATRP graft polymerizations have occurred throughout the cellulose acetate fiber surfaces.

Thermal stabilities: Non-isothermal TGA under nitrogen atmosphere was used to characterize the thermal stability of cellulose acetate, CA-*g*-PAA and CA-*g*-PAM. The results are shown in Fig. 6. The decomposition of cellulose acetate started at about 331 °C. The maximum decomposition temperature of cellulose acetate is around 383 °C. However, the TGA profile of CA-*g*-PAA and CA-*g*-PAM are distinctly different from that of cellulose acetate. After the graft, T5 % decreased to 257 and 307 °C for CA-*g*-PAA and CA-*g*-PAM, respectively and with a maximum decomposition temperature around

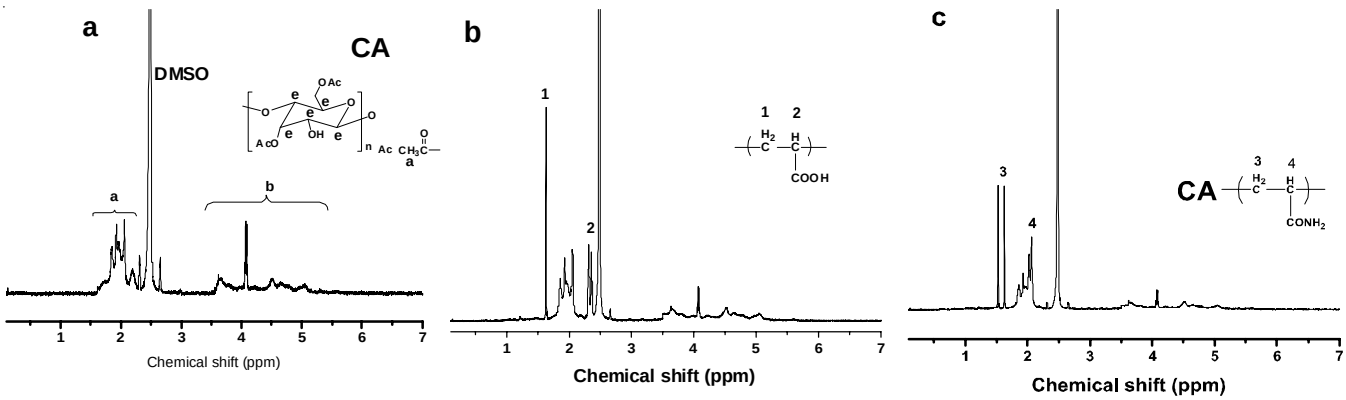

Fig. 3. ^{1}H NMR spectrum of (a) cellulose acetate fiber, (b) CA-*g*-PAA and (c) CA-*g*-PAM

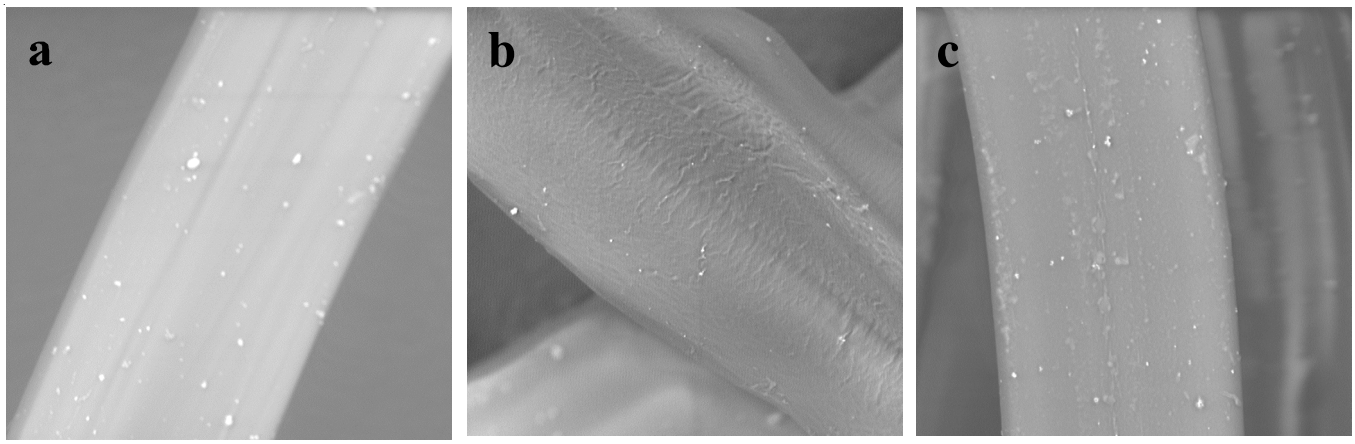

Fig. 5: SEM images of (a) cellulose acetate fiber, (b) the CA-*g*-PAA and (c) CA-*g*-PAM (magnified by 5000 times)

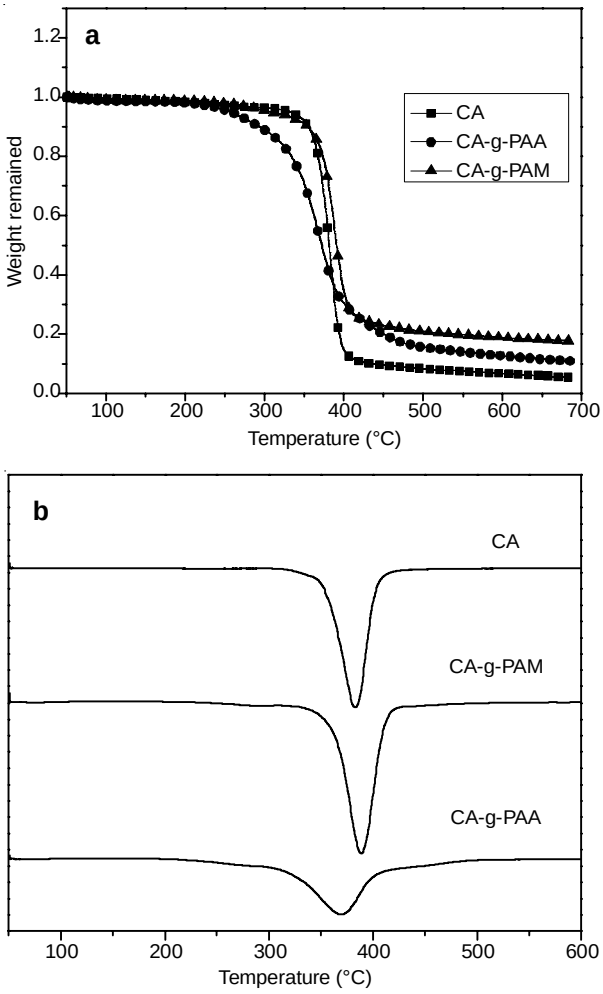

Fig. 6. TGA (a) and DTGA (b) curves of cellulose acetate, the CA-*g*-PAA and CA-*g*-PAM

370 and 389 °C are the thermal degradation for CA-*g*-PAA and CA-*g*-PAM, respectively. So, from the TGA analysis, it demonstrated that the thermal stability of cellulose acetate copolymers is changed by the graft.

Kinetics of ATRP grafting process: The kinetics of poly-(acrylic acid) and polyacrylamide growth from the cellulose acetate-Br fiber *via* surface-initiated ATRP was investigated. The grafting yield (GY) was determined gravimetrically, the graft concentration can be defined as following:

$$GY = \frac{\text{Weight of cellulose acetate-}g\text{-PAA or cellulose acetate-}g\text{-PAM-Weight of cellulose acetate-Br}}{\text{Weight of cellulose acetate-Br}}$$

Fig. 7(a,b) show the dependence of the grafting yield on the ATRP time and monomer concentration, respectively. It can be seen that the grafting yield increases with polymerization time for modification less than 4 h and it reaches a platform

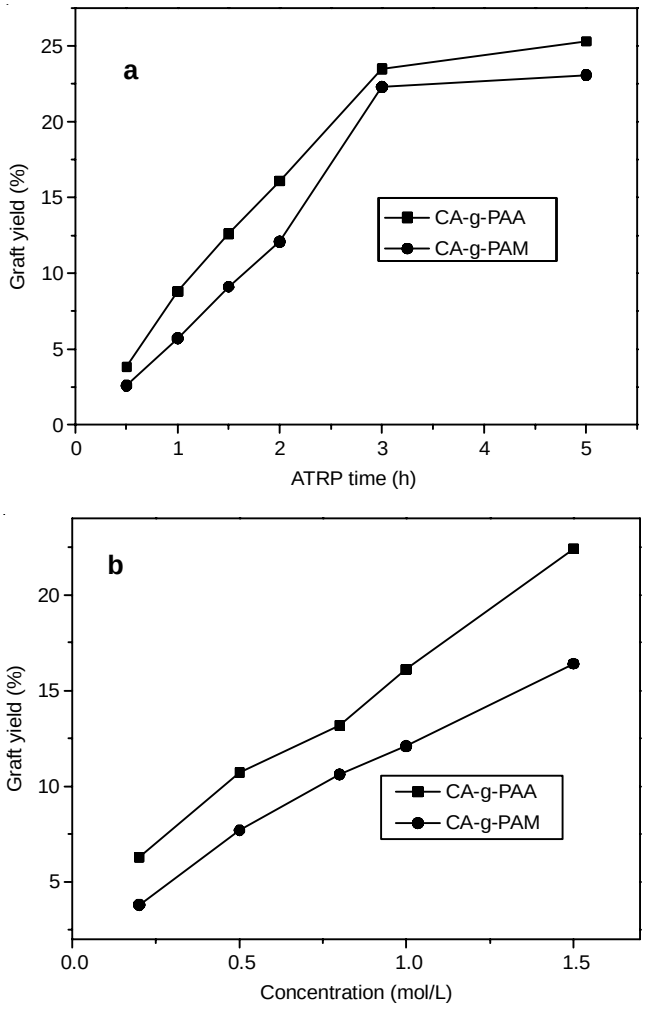

Fig. 7. Dependence of graft yield of the CA-*g*-PAA and CA-*g*-PAM on: (a) the surface-initiated ATRP time, and (b) the monomer concentration

form grafting yield for longer polymerization times. The results suggest that the chain growth from the cellulose acetate-Br fiber is consistent with a living and well-defined process. The nonlinear growth behaviour has been showed for other polyacids, results from chain termination reactions, as well as catalyst deactivation[16]. The relationship between the grafting yield and the monomer concentration is shown in Fig. 7(b). An approximately linear increase in degree of grafting of the poly(acrylic acid) and polyacrylamide chains on the cellulose acetate-Br fiber with the monomer concentration, suggest that the growth of the chains was a controlled process, which is consisted with the results reported by Sankhe *et al*.[17]. In the same condition, cellulose acetate fiber has used to contrast test, the results suggest that the cellulose acetate fiber can not initiated ATRP polymerization. All of these results are consistent with the successful graft polymerization of acrylic acid and acrylamide on the CA-Br fiber *via* surface-initiated ATRP.

Conclusion

A surface-initiated ATRP modification method was developed for CA-Br fiber graft. Well-defined functional polymer polyacrylic acid and polyacrylamide was covalently grafted onto the surface of the CA-Br fiber *via* surface-initiated ATRP. The kinetics study revealed an approximately linear increase in the graft yield of the poly(acrylic acid) and polyacrylamide with polymerization concentration, indicating that chain growth from the fiber surface was consistent with a controlled process. The surface functionality of CA-Br fiber could be precisely tailored in a controlled manner.

ACKNOWLEDGEMENTS

The authors acknowledge the financial support from Science and Technology program of China Tobacco Yunnan Industrial Co., Ltd. (2013FL05).

REFERENCES

1. D. Aoki, Y. Teramoto and Y. Nishio, *Biomacromolecules*, **8**, 3749 (2007).
2. M. Bertoldo, G. Zampano, F.L. Terra, V. Villari and V. Castelvetro, *Biomacromolecules*, **12**, 388 (2011).
3. Y. Cao, J. Wu, T. Meng, J. Zhang, J. He, H. Li and Y. Zhang, *Carbohydr. Polym*., **69**, 665 (2007).
4. Y. Cao, H. Li and J. Zhang, *Ind. Eng. Chem. Res*., **50**, 7808 (2011).
5. W.J. Deng, X.P. Zhuang, K.T. Guan and B.W. Cheng, *Adv. Mater. Res*., **221**, 85 (2011).
6. G.A. El Seoud, G.A. Marson, G.T. Ciacco and E. Frollini, *Macromol. Chem. Phys*., **201**, 882 (2000).
7. Y. Enomoto-Rogers, H. Kamitakahara, T. Takano and F. Nakatsubo, *Biomacromolecules*, **10**, 2110 (2009).
8. S.C. Fox, B. Li, D. Xu and K.J. Edgar, *Biomacromolecules*, **12**, 1956 (2011).
9. K.C. Gupta, S. Sahoo and K. Khandekar, *Biomacromolecules*, **3**, 1087 (2002).
10. Y. Luan, J. Wu, M. Zhan, J. Zhang, J. Zhang and J. He, *Cellulose*, **20**, 327 (2013).
11. M.L. Hassan, R.M. Rowell, N.A. Fadl, S.F. Yacoub and A.W. Christainsen, *J. Appl. Polym. Sci*., **76**, 561 (2000).
12. K.J. Edgar, C.M. Buchanan, J.S. Debenham, P.A. Rundquist, B.D. Seiler, M.C. Shelton and D. Tindall, *Prog. Polym. Sci*., **26**, 1605 (2001).
13. G.S. Luo, M. Niang and P. Schaetzel, *Sep. Sci. Technol*., **32**, 1143 (1997).
14. M. Rahman and C.S. Brazel, *Prog. Polym. Sci*., **29**, 1223 (2004).
15. Y. Teramoto and Y. Nishio, *Biomacromolecules*, **5**, 407 (2004).
16. Y. Teramoto and Y. Nishio, *Biomacromolecules*, **5**, 397 (2004).
17. A.Y. Sankhe, S.M. Husson and S.M. Kilbey, *Macromolecules*, **39**, 1376 (2006).
18. S. Chen, G. Wu, Y. Liu and D. Long, *Macromolecules*, **39**, 330 (2006).
19. Z. Xu, Y. Yang, Y. Jiang, Y. Sun, Y. Shen and J. Pang, *Molecules*, **13**, 490 (2008).